

Near-threshold effects in the ionization of atoms (the post-collision interaction)

M. Ya. Amus'ya, M. Yu. Kuchiev, and S. A. Sheĭnerman

A. F. Ioffe Physicotechnical Institute of the Academy of Sciences of the USSR
(Submitted 18 February 1978)
Zh. Eksp. Teor. Fiz. 76, 470-481 (February 1979)

A special class of phenomena occurring in the inelastic scattering of electrons by atoms is investigated assuming that the energy of the incident electron is close to the excitation threshold of the autoionizing state. It is shown that the interaction between a slow electron and the vacancy in the final state (the so-called post-collision interaction) has an appreciable effect on the characteristics of the process. Acceptable agreement with the available experimental data can be obtained by taking into account to the post-collision interaction in calculations for specific processes.

PACS numbers: 34.80.Dp, 34.10. + x

1. A very interesting phenomenon appears in studying electron scattering by helium atoms when the incident electron energy is slightly greater than the energy of the autoionizing state.¹ It turns out that the energy of the electron emitted after the decay of the autoionizing state depends on the energy of the incident electron. The shape of the line corresponding to this autoionizing state in the ejected-electron spectrum also depends on the energy of the incident electron. In the literature this effect has been called the "post-collision interaction" (PCI). A qualitative explanation of it is that the incident electron loses almost all its energy in exciting the autoionizing state and then slowly leaves the atom. If the velocity of this "slow" electron is sufficiently small, its field will affect all the characteristics of the decay of the autoionizing state; the effect will be greater the closer the slow electron is to the atom at the time of the decay, that is, the lower its velocity. The PCI effect is manifested the more strongly, the shorter the lifetime of the excited state, that is, the broader the level. If the level width is comparable with the energy of the slow electron, it is not possible to assign a definite energy to this electron. In this case the excitation and decay of the autoionizing state form a single process which cannot be viewed as occurring in two stages.

The PCI effect can appear not only in the inelastic scattering of relatively slow electrons, but also in other ionization processes. As an example, if the photon energy is slightly greater than the photoionization threshold of an inner shell, then in the absorption of this photon a hole and a slow electron are produced; this electron plays an important role in the subsequent Auger or radiative decay of the inner vacancy. The energy of the Auger electron near the ionization threshold therefore depends on the photon frequency.²

As we show in the present study, the interaction of the charged particles is in the final state very important for describing the effects mentioned above. There are three of these particles: the slow electron, the ion, and a fast electron which comes from the decay of the excited state. The interaction between the fast electron and the other two particles is small and can be neglected compared to that between the slow electron and the ion.

Therefore, the three-body problem actually reduces to taking into account the effect of the ion field on the slow electron. As will be shown below, this interaction is very important and leads to a redistribution of the energy between the electrons: the slow one slows down and the fast one speeds up. This result is the opposite of that in the Wannier process,³ where there are also two electrons and an ion in the final state, but their interaction tends to equalize the electron energies. The difference arises from the fact that in the Wannier process both electrons are slow and the interactions between all three particles must be taken into account, whereas only the slow electron and the ion effectively interact in the case we are considering here.

In the present study the excitation of an autoionizing state or a vacancy and their decay is viewed as a unified process for the first time. This makes it possible not only to describe the energy shift due to the PCI, but also to calculate the cross section for the process. In section 2 of this study we give the most important graphs of many-body theory which describe the interaction between the slow electron and the atomic particles. In section 3 we show qualitatively that the inclusion of these graphs causes the line corresponding to the autoionizing state in the spectrum of the knocked out electrons to change: the line is shifted and broadened and becomes asymmetric the more, the closer the incident electron energy is to the excitation threshold of the autoionizing level. In addition, oscillations appear at the line edges. In section 4 we consider the PCI for the example where singly charged Ar^+ ions are produced when the energy transferred to the atom is close to the $2p^6$ -subshell ionization threshold. We show that the PCI effect causes a maximum to appear in the cross section for this process at the reaction threshold; the calculated absolute cross section and shape of the peak are in satisfactory agreement with the experimental data.⁴ In section 5 we consider a different example of the PCI: the scattering of an electron on an Ar atom near the threshold of the autoionizing level $3s4p(3P)$. It is shown that the PCI effect is manifested not only in a change of the energy, but also in the angular distribution of the slow electrons.

2. The simplest graph describing the excitation of a

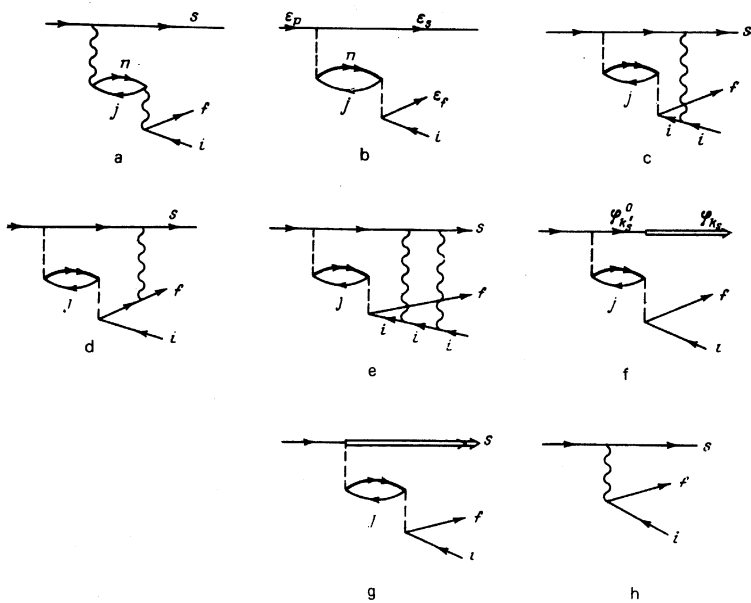


FIG. 1.

single-particle autoionizing level by electron impact and its subsequent decay is shown in Fig. 1a. The narrow line with the arrow to the right (left) describes the electron (hole) propagation, the line with the double arrow corresponds to an electron in an excited discrete level, and the wavy line corresponds to the Coulomb interaction. Below we shall use the usual rules for associating the graphs with analytic expressions.⁵

The graph of Fig. 1a is a resonance graph, because the energy denominator corresponding to the virtual excitation of the autoionizing level becomes zero when the energy transferred to the atom by the incident electron equals the excitation energy of the discrete level. It is therefore necessary to sum the contributions of all the resonance graphs in the higher orders of perturbation theory. We must take into account the possibility of the decay of the autoionizing state, which leads to the imaginary contribution $i\Gamma/2$ (Γ is the width of the level) to the energy of the autoionizing state. In addition, the excitation and decay of this discrete state can proceed via virtual excitation of some other atomic configurations. We shall include these processes by introducing an effective interaction U instead of the Coulomb interaction.

Summation of all the resonance diagrams leads to Fig. 1b, in which the dashed lines denote the interaction U and the heavy line of the discrete state indicates the inclusion of the level width. The analytic expression for the amplitude $A_0(k_s)$ of the process represented by this graph is

$$A_0(k_s) = \frac{\langle k_s, n | U | p, j \rangle \langle j, k_f | U | n, i \rangle}{\varepsilon_p - \varepsilon_s - E_{ex} + i\Gamma/2}. \quad (1)$$

Here ε_p is the energy of the incident electron, k_s and ε_s are the momentum and energy of the slow electron s , k_f and ε_f are the momentum and energy of the fast (compared to s) electron f , E_{ex} , and Γ are the excitation energy and width of the autoionizing level, E_i is the energy of the hole i , and n and j denote the states of the electron and hole forming the autoionizing level. The ener-

gies of the incident and departing electrons satisfy the conservation law

$$\varepsilon_p = \varepsilon_s + \varepsilon_f + E_i. \quad (2)$$

If near the resonance we can neglect the energy dependence of the matrix elements on the right-hand side of (1), then, taking (2) into account, $A_0(k_s)$ describes a Lorentz line of width Γ in the ejected-electron spectrum with maximum at

$$\varepsilon_f = E_{ex} - E_i. \quad (3)$$

Let us now consider the interaction of the slow electron with the fast electron and the hole produced as a result of the decay of the autoionizing level. This is a three-body problem. We are, however, interested in the case when one of the electrons is fast, and its interaction with the other electron is insignificant. In fact, a direct estimate of the graphs in Figs. 1c and d shows that if

$$k_s \ll 1 \ll k_f \quad (4)$$

(here we use atomic units $\hbar = m = e = 1$) the contribution of graph d can be neglected compared to that of c . This result has a simple physical explanation: the fast electron ejected in the decay of the autoionizing state does not manage to interact with the slow one.

Henceforth we will assume that the condition (4) is satisfied and take into account only the final-state interaction between the slow electron and the hole i . This interaction must be taken into account exactly, since perturbation theory is not applicable because of the low electron energy.

We also need to consider the interaction between the slow electron and the field of the virtual autoionizing state. However, according to the well known technique in Ref. 6, we can do this by using the Hartree-Fock wave function $\varphi_{k_s}^0$ of the slow electron in the field of the excited atom. The narrow line corresponding to the slow electron s in Fig. 1b implies its motion in this field. Let us now take into account the interaction between the slow electron and the vacancy i in the final state by

summing a "ladder" of graphs similar to that in Fig. 1e. Letting $A(k_s)$ denote the contribution of the sum of these graphs, we find

$$A(k_s) = \int A_o(k_s') \langle \varphi_{k_s} | \varphi_{k_s'}^0 \rangle dk_s', \quad (5)$$

where φ_{k_s} is the wave function of the slow electron in the field of the hole i . With (5) we can associate the graph of Fig. 1f, in which the double line denotes the electron moving in the field with the hole i , and the junction of the narrow line and the double line denotes the overlap integral $\langle \varphi_{k_s} | \varphi_{k_s'}^0 \rangle$. Below we will consider the region where (5) is applicable.

The amplitude (5), obtained using the condition (4), describes the instantaneous decay of the autoionizing state, whereby the slow electron feels a sudden change in the field. We will use a similar method for taking into account the sudden field change in other processes in which a slow electron and an autoionizing state are produced. For example, in the photoionization of an inner shell an electron and a vacancy then undergoes Auger decay. This process is shown in Fig. 2a. Near the photoionization threshold the main correction to this graph, just as in the earlier case, comes from the final-state interaction between the electron and the ion field, which is accounted for by the diagram in Fig. 2b. The narrow line for the slow electron describes its motion in the field of the inner vacancy l and the double line devotes the wave function in the combined field of the holes i and j .

3. We shall show that the graph of Fig. 1f leads to a shift of the maximum and a change in the shape of the autoionizing line in the Auger electron spectrum. For simplicity we consider only the case $\Gamma \ll 1$. For this case, as shown below, the slow electron in the final state is localized outside the atom and the problem is greatly simplified. Interchanging the order of the integration over the coordinate (the overlap integral) and over the energy in (5), we obtain

$$A(k_s) = \int \varphi_{k_s}^*(r) \varphi(r) dr, \quad (6)$$

where $\varphi_{k_s}(r)$ is the wave function of the final state and, according to (1), $\varphi(r)$ is given by the expression

$$\varphi(r) = \int \frac{\langle r | \varphi_{k_s}^0 \rangle \langle k_s, n | U | p, j \rangle}{\epsilon_p - E_{ex} - \epsilon_s + i\Gamma/2} dk_s \langle j, k_f | U | n, i \rangle. \quad (7)$$

In the matrix element $\langle k_s, n | U | p, j \rangle$ the index k_s denotes the wave function of the slow electron in the intermediate state $\varphi_{k_s}^0$. (The matrix element $\langle j, k_f | U | n, i \rangle$ depends weakly on k_s in the resonance region of interest to us and we have taken it outside the integral sign.) The integration over k_s in (7) can therefore be carried out using the retarded Green's function describing the propagation of the slow electron in the field of the ex-

cited atom. Using the asymptotic properties of the Green's function,⁷ we find from (7)

$$\varphi(r) \rightarrow A_o(k_o) \frac{e^{ik_o r}}{r} + O\left(\frac{1}{r^2}\right), \quad r \rightarrow \infty, \quad (8)$$

where the momentum k_o has a real and an imaginary part:

$$k_o = k_1 + ik_2 = [2(\epsilon_p - E_{ex}) + i\Gamma]^{1/2} \quad (9)$$

and A_o is in the inelastic scattering amplitude (1) without the PCI. The first term in (8) is a "diverging" wave. Allowance for the finite level width causes the wave to be exponentially damped, as a result of which the diverging wave is localized in the region $r \approx 1/k_2$. For $\Gamma \ll 1$ this region exceeds the size of the atom: $1/k_2 \gg 1$ and, in addition, here the terms $O(1/r^2)$ are smaller than the diverging wave and can be neglected.

Therefore, the main contribution to the integral (6) comes from distances $1 < r < 1/k_2$, where the function $\varphi(r)$ is approximated well by the first term on the right-hand side of (8). At these distances the motion of the slow electron in the Coulomb field is semiclassical. Consequently, the overlap integral (6) can be calculated using the stationary phase method.⁸

Using the argument of the Coulomb function as the argument of the function $\varphi_{k_s}(r)$ of the electron in the continuum, we find that $|A(k_s)|$ has a maximum when

$$\epsilon_s = k_1^2/2 - k_2. \quad (10)$$

We see that when the PCI is taken into account the maximum of the modulus of the amplitude is shifted by an amount $\delta\epsilon_s = -k_s$, as first noted in Ref. 9. Since we are everywhere assuming that the energy conservation law (2) is satisfied, the spectral-line maximum corresponding to the autoionizing level is shifted by $\delta\epsilon_f = k_2$. Thus, the PCI leads to a redistribution of the energy between the electrons: the fast one speeds up and the slow one slows down. This result is not surprising; in fact, the energy exchange between the electrons occurs not as a result of their direct interaction (the graph of Fig. 1d is small), but is a consequence of the attraction between the slow electron and the ion. We note that with increasing k_s the argument of the Coulomb function changes more than when k_s is decreased. Because of this, first of all, the overlap integral (6) falls off more smoothly in the direction of smaller k_s . Therefore, as a result of the PCI the shape of the autoionizing line in the Auger spectrum becomes asymmetric: for larger ϵ_f (smaller ϵ_s) the line falls off more slowly than the Lorentz line neglecting the PCI, while for small ϵ_f it falls off more rapidly than the Lorentz line. Secondly, we conclude that the broadening of one side of the line is more marked than the narrowing of the other, so that on the whole the line is broadened.

The phenomena discussed above, that is, the autoionizing line shift, its broadening, and its asymmetry, are all related to the addition of a quantity determined by the Coulomb field of the ion to the argument of the function $\varphi_{k_s}(r)$. The quantity is larger, the lower the energy of the slow electron. These phenomena are therefore manifested more clearly in the near-threshold region.

Up to this time we have taken into account only the

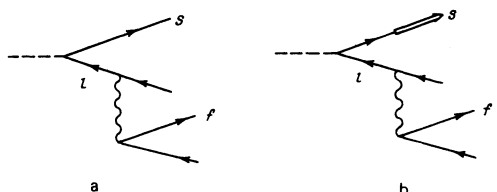


FIG. 2.

amplitude of the resonance process. Let us now consider what complications appear due to interference between the resonance and phonon amplitudes (the simplest nonresonance phonon graph is shown in Fig. 1h). Neglecting the PCI, the phase of the resonance amplitude changes by π in the resonance region, which causes the cross section to acquire the characteristic Fano profile.¹⁰

Let us now take into account the effect of the PCI on the phase of the amplitude $A(k_s)$. For this we shall use the asymptotic expression (8) for the function $\varphi(\mathbf{r})$ and we shall approximate the final-state wave function $\varphi_{k_s}(\mathbf{r})$ by a Coulomb function. Both of these approximations are always valid for an estimate, since the region where the electron is localized $r \sim 1/k_2$ exceeds the size of the atom at $k_2 \ll 1$. Then for $A(k_s)$ we find from (6)

$$A(k_s) = a \frac{e^{\epsilon_1 + i\epsilon_2}}{\epsilon_p - E_{ex} - \epsilon_{k_s} + i\Gamma/2}, \quad (11)$$

where

$$\varphi_1(k_s) = -\frac{1}{k_s} \operatorname{arctg} \frac{2k_s k_2}{k_1^2 + k_2^2 - k_s^2},$$

$$\varphi_2(k_s) = \frac{1}{2k_s} \ln \frac{(k_s - k_1)^2 + k_2^2}{(k_s + k_1)^2 + k_2^2},$$

k_1 and k_2 are given in (9), and the coefficient a depends weakly on k_s . Expression (11) was obtained earlier (see Ref. 11) on the basis of a quasimolecular adiabatic consideration of the PCI.

We see that the PCI adds to the phase of $A(k_s)$ the quantity $\varphi_2(k_s)$, which can vary greatly in the resonance region. (For example, for $\epsilon_p - E_{ex} = 1$ eV and $\Gamma = 0.1$ eV, $\varphi_2(k_s)$ is $\sim \pi$ when ϵ_s is changed from 1.0 eV to 1.1 eV.) When the phase $\varphi_2(k_s)$ is changed by π in the resonance region the autoionizing line contour acquires an additional maximum and minimum. We therefore see that the PCI leads to an oscillatory structure in the autoionizing line profile. To observe these oscillations it is necessary that the energy spread of the incident electrons be less than the width of the autoionizing level.

Up to now we have considered the slow electron in the continuum in the final state of the reaction. The decrease in the energy of the slow electron can be sufficient for it to fall into a bound state, i.e., an excited atom is produced in the final states. An investigation similar to that above shows that in this case the characteristic manifestations of the PCI in the spectrum of the knocked-out electrons remain unchanged: the autoionizing line shifts, becomes asymmetric, and broadens, while oscillations appear at the edges of the line. The calculations according to (1) and (6) are simpler for transitions to discrete states. If the wave function of the discrete state falls off faster than $\varphi(\mathbf{r})$ (for this we must have $k_2 < \kappa_n$, where $\kappa_n = \sqrt{-2E_n}$ with E_n the energy of the discrete state), then according to (6) and (8) we can neglect the width of the level.

The problem of how the PCI affects the cross section for the production of an excited atom is very interesting. Resonance scattering with the production of an excited atom can also occur when the PCI is neglected, as shown in the graph of Fig. 1g. The cross section of the process in this graph is resonant; neglecting the PCI, the in-

crease in the yield of excited atoms at the resonances $\epsilon_p = E_{ex} + E_s$ ($E_s < 0$ is the energy of the discrete state) has a width equal to that of the autoionizing level, while the resonances themselves are distributed up to the excitation threshold. The inclusion of the PCI changes this situation. The PCI causes the energy of the slow electron to decrease, so it can fall into a discrete level even if the incident electron energy exceeds the reaction threshold. Thus an increase in the yield of neutral atoms must occur beyond the reaction threshold. The calculation given below confirms this.

We have studied the consequences of taking into account the graph of Fig. 1f for the case of inelastic scattering. We made a similar study for the graph of Fig. 2b also, which describes the PCI in the near-threshold photoionization of an inner shell. All the main conclusions about the knocked-out electron spectrum remain valid in the case of the line corresponding to Auger decay. In this case the discrete states of the slow electron correspond to the excited levels of the singly charged ion and the PCI must have a substantial effect on the cross section for the yield of such ions.

All the results of this section were obtained for $\Gamma \ll 1$. However, formula (5), which is the basis of our investigation, does not need this assumption. The conclusion (5), except for the inequality (4), is based on the requirement that the contribution to the cross section of the discarded nonresonance graphs, for example, that of Fig. 1h, be separable from the contribution of the resonance graphs that were included. For this it is sufficient only that the width Γ be smaller than the energy range in which the nonresonance amplitude changes significantly, i.e., $\Gamma \ll \epsilon_f$. In the case $\Gamma \sim 1$, as seen from (8) and (9), the slow electron is localized at distances $r \sim 1$ and simple estimates of the wave functions are inapplicable. Therefore, in this case it is not possible to obtain explicit formulas for the change of the line shapes as a function of the incident electron energy. It can, however, be rigorously shown (this is done in the Appendix) that in this case the PCI causes the line to shift.

4. Let us consider the cross section for the yield of singly charged Ar^+ ions in the inelastic scattering of a fast electron by an Ar atom when the energy ω transferred to the atom is close to the $2p^6$ -subshell ionization threshold. According to section 2, in this case the PCI is included via the diagram of Fig. 3, in which the narrow line corresponds to the slow electron moving in the field of the hole $2p$ and the double line corresponds to the combined field of the two holes.

The differential cross section for the single ionization of the atom by the fast electron is related to the density of the generalized oscillator strengths $F(q, \omega)$ (Ref.

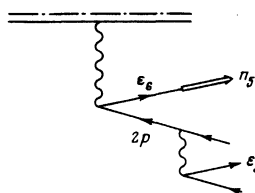


FIG. 3.

12). After integrating over the angles and summing over the spin projections, the quantity $F(q, \omega)$ corresponding to the graph in Fig. 3 has the form

$$F = \sum_p 4\omega \frac{3(2l_s+1)}{2p+1} \begin{pmatrix} l_s & l_1 & 1 \\ 0 & 0 & 0 \end{pmatrix}^2 \quad (12)$$

$$\times \left| \langle n_1 l_1, \varepsilon_3 l_3 \| V_p \| n_2 l_2, n_4 l_4 \rangle \sum_{\varepsilon_6} \frac{B_{n_1 l_1 \rightarrow \varepsilon_6 l_5}(q) \langle \tilde{n}_5 l_5 \| \varepsilon_6 l_5 \rangle}{\omega - \varepsilon_6 + \varepsilon_{n_1 l_1}} \right|^2$$

where p is the orbital angular momentum transferred in the Auger decay, $\langle \tilde{n}_5 l_5 \| \varepsilon_6 l_5 \rangle$ is the overlap integral of the radial Hartree-Fock wave functions of particles located in different self-consistent fields, $\langle \| V_p \| \rangle$ is the reduced matrix element of the Auger decay, and $B_{n_1 l_1 \rightarrow \varepsilon_6 l_5}(q)$ is the reduced matrix element of the transition $n_1 l_1 \rightarrow \varepsilon_6 l_5$ under the influence of the fast incident electron. The summation over ε_6 includes the integration over all possible states of the discrete and continuous spectra. Only dipole transitions are included in (12), since everywhere below we consider small momenta q transferred to the atom by the incident fast electron. The slow electron can therefore be in s or d states. In deriving (12) we have neglected the width of the $2p$ level in accordance with the considerations of section 3.

For the wave functions of the knocked-out fast electron in the $\varepsilon_3 l_3$ state we used the Hartree-Fock wave functions $\varphi^i(MLS)$ calculated in the field of the frozen core with hole i (Ref. 6) (since the other hole is screened by the electron in the discrete level). The Hartree-Fock functions of the electron in the intermediate state $\varepsilon_6 l_5$ are calculated in the field of the completely rearranged core with a hole in the $2p$ state. The wave functions of the electron in discrete states ns or nd are determined using the self-consistent configuration taking into account the presence of the two holes in the states k_2 and k_4 .

Calculation shows that the probability for processes with electron transitions into discrete ns levels are on the average two orders of magnitude smaller than the corresponding processes with transitions into discrete nd levels. We calculated the probability for electron transitions into the first eight discrete d levels. The calculated dipole component of the density of the generalized oscillator strengths for processes including the PCI are shown in Fig. 4. As expected, the inclusion of the correlations due to the PCI causes the yield of singly charged ions to increase sharply at the $2p^6$ -subshell threshold. The width of the resulting peak is ~ 2.5 – 3 eV. In this figure we also give the experimental curve for the singly charged ion yield (dashed line), extracted from the measurements of Van der Wiel et al.⁴ Here the experimental curve for the energy losses, given in

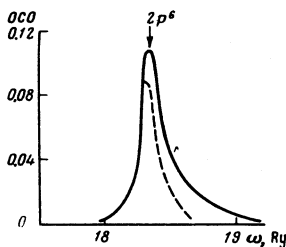


FIG. 4.

relative units, was normalized by us so that the experimental maximum of the $2p^6$ -subshell ionization given in Ref. 13 would coincide with the calculated maximum. The figure shows that the agreement between theory and experiment is satisfactory. Since this agreement results only from including the PCI, we can take this as proof that the PCI plays an important role in the production of Ar^+ ions at the L -shell threshold. The possibly important role of the PCI in this case was also mentioned in Ref. 4. Other mechanisms for producing Ar^+ ions at the L -shell threshold, in particular, direct ionization of the M shell and ionization of the M shell under the influence of the L shell, were discussed in Ref. 14. Compared to the PCI processes that we have studied, the contributions of these mechanisms to the production of Ar^+ ions at the L -shell threshold are insignificant.

5. Let us now consider a specific calculation of the PCI effect in the case where the slow electron in the final state is in the continuum. For this we studied the inelastic scattering of an electron on an Ar atom with the excitation of the autoionizing state $3s4p(^3P)$ for an incident electron energy close to the excitation threshold (26.46 eV) of this level. As shown in sections 2 and 3, in this process the PCI effects is described by the diagram of Fig. 1f. In this case (a triplet autoionizing state) we need to take into account only the exchange graph shown in Fig. 5. We calculated this graph using formulas (1) and (5).

As the wave functions of the slow electron in the final state we used the Hartree-Fock wave functions calculated in the field of the rearranged core with a $3p$ hole. The wave functions of the slow electron in the intermediate state were calculated in the field of the excited state. The functions of the incident electron were found in the field of the frozen atom, while those of the autoionizing electron were taken in the field of the core with the $3p$ hole.

The main difficulty in calculating the graph in Fig. 5 is that in the intermediate stage it is necessary to find the overlap integral of wave functions of the slow electron belonging to different continuous spectra [see (5)]. We need the finite cutoff radius $R = 100$ for these wave functions. For a fixed energy ε_{k_3} the overlap integral changed rapidly as a function of the intermediate electron energy $\varepsilon_{k'}$, in the region $\varepsilon_{k'} \approx \varepsilon_{k_3}$. Therefore, in integrating over k' (see (5)) it was necessary to choose enough of the wave functions of the intermediate slow electron.

Calculation shows that the matrix element of the Auger decay $\langle 3s, \varepsilon_f l_f \| V \| 3p, 4p \rangle$ with a transition to the state with $l_f = 2$ considerably exceeds the matrix element of the transition to an s state and weakly depends on the energy of the autoionizing electron ε_f in the ener-

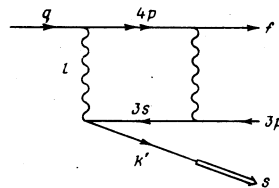


FIG. 5.

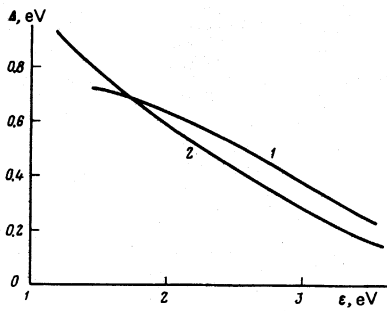


FIG. 6.

gy range of interest to us. In lowest order perturbation theory this matrix element determines the width of the autoionizing level:

$$\Gamma = \frac{4}{3\pi} |\langle 3s, \epsilon, d \| V \| 3p, 4p \rangle|^2,$$

which is ≈ 0.2 eV. In the subsequent calculations this quantity determined the imaginary part of the energy denominator in (1).

The diagram of Fig. 5 was calculated with the slow electron angular momenta $l_q = 0, 1, 2$. Large angular momenta clearly cannot play a significant role, since we are considering the process near threshold. Calculation shows that the matrix elements of the inelastic scattering $\langle \epsilon_k, l_s, 4p \| V \| 3s, ql_q \rangle$ behave in the usual manner: at the threshold itself only a monopole transition is possible for $\epsilon_k = 0$, while with increasing ϵ_k , both dipole and quadrupole transitions appear (thus, for example, already at $\epsilon_k = 5$ eV the reduced matrix element of the quadrupole transition reaches the same value as that of the monopole transition). Therefore, if the PCI were neglected the angular distribution of the slow electrons at threshold would be isotropic, that is, the anisotropy coefficient β in the expression for the differential cross section

$$\sigma(\theta) = \sigma_0(1 + \beta P_2(\cos \theta))$$

would be zero. Our calculation showed that in the graph of Fig. 5 the overwhelming contribution comes from only the quadrupole transition in the entire near-threshold region. This corresponds to $\beta = +1$. Therefore, in this process the PCI has a sizeable effect on the angular distribution of the slow electrons.

The amplitude of Fig. 5 was used to calculate the differential cross section for inelastic resonance scattering with the production of a singly charged ion. For fixed incident electron energy we determined the maximum of the cross section viewed as a function of the Auger electron energy. Figure 6 shows the resulting dependence of the energy shift Δ of the Auger electron as a result of the PCI on the incident electron energy ϵ , measured from the excitation threshold of the autoionizing level (curve 1). In the same figure we show the experimental dependence (curve 2) obtained in Ref. 15, where the total cross section for producing both the Ar^+ ion and the excited atom Ar^* was measured. The figure shows that the experimental and theoretical curves are in satisfactory agreement for $\epsilon > 1$ eV. A difference appears at lower energies due to the fact that in this region the energy shift due to the PCI becomes comparable to the energy of the slow electron. The slow electrons therefore fall mainly into discrete levels in

the final state (see section 4). These transitions were taken into account in the experimental cross sections and gave the dominant contribution for $\epsilon \rightarrow 0$. They did not, however, contribute to the cross section for scattering with Ar^+ production that we studied.

6. In the present study we have developed a quantitative quantum mechanical theory of the PCI phenomenon based only on the single assumption that the change of the field in which the slow electron moves occurs in such a small time interval that the interaction between the fast and the slow electron can be neglected. We have shown for specific examples that it is possible to carry out numerical calculations which can be directly compared to the experimental results. We have illustrated almost all of the possible manifestations of the PCI: the shift of the maximum in the energy distribution of the fast (or slow) electrons, the asymmetry of the shape of the line and its broadening, and the change in the angular distribution of the slow electrons. Unfortunately, it has not been possible to take into account the interference between the resonance and phonon amplitudes in specific calculations because the accuracy of calculating the resonance amplitude is not yet good enough.

In the future we plan to use this calculational technique to study the PCI in the case of broader (of order 1 eV) autoionizing levels, where the PCI effect can be even more pronounced.

In conclusion the authors are grateful to L. V. Chernysheva for letting them use her computer programs for the numerical calculations.

APPENDIX

We shall show in the general case that the PCI leads to a shift of the line corresponding to the excited state in the ejected electron spectrum. The differential cross section for the inelastic scattering is proportional to $|A(k_s)|^2$, where the amplitude $A(k_s)$ is given by expression (5). Let us define the average energy of the slow electron as the cross section average:

$$\bar{\epsilon}_s = \frac{\int \epsilon_s d\sigma(\epsilon_s)}{\int d\sigma(\epsilon_s)} = \frac{\int \epsilon_s |A(k_s)|^2 dk_s}{\int |A(k_s)|^2 dk_s}.$$

The mean energy of the fast electron is given by the conservation law (2). Using (6) we can change the expression for the mean energy to the form

$$\epsilon_s = \langle \varphi | \hat{H} | \varphi \rangle / \langle \varphi | \varphi \rangle,$$

where $\varphi(\mathbf{r})$ is given in (7) and \hat{H} is the Hamiltonian describing the final-state motion of the slow electron. In deriving the latter equation we have taken into account the fact that the functions φ_{k_s} [see (5)] are the eigenfunctions of the operator \hat{H} . Similarly, when we neglect the PCI we find

$$\bar{\epsilon}_s^{(0)} = \langle \varphi | \hat{H}_0 | \varphi \rangle / \langle \varphi | \varphi \rangle,$$

where \hat{H}_0 is the Hamiltonian describing the motion of the slow electron in the field of the autoionizing state. Thus the energy shift due to the PCI is

$$\delta \epsilon_s = -\delta \epsilon_f = \epsilon_s - \bar{\epsilon}_s^{(0)} = \langle \varphi | \hat{H} - \hat{H}_0 | \varphi \rangle / \langle \varphi | \varphi \rangle = \langle \varphi | V | \varphi \rangle / \langle \varphi | \varphi \rangle, \quad (13)$$

where $V = \hat{H} - \hat{H}_0$ is the change of the Hamiltonian due to

the decay of the excited state. The potential V is attractive, so that its mean value is negative. Therefore, the energy of the slow electron is decreased and that of the fast electron is increased.

¹P. J. Hicks, S. Cvejanović, J. Comer, F. H. Read, and J. M. Sharp, *Vacuum* **24**, 573 (1974).

²F. H. Read, *Radiat. Res.* **64**, 23 (1975).

³G. H. Wannier, *Phys. Rev.* **90**, 817 (1953).

⁴M. J. Van der Wiel, G. R. Wight, and R. R. Tol, *J. Phys. B: Atom. Molec. Phys.* **9**, L5 (1976).

⁵A. A. Abrikosov, L. P. Gor'kov, and I. E. Dzyaloshinskiĭ, *Metody kvantovoi teorii polya v statisticheskoĭ fizike*, Fizmatgiz, 1963 (Engl. transl. *Methods of Quantum Field Theory in Statistical Physics*, Englewood Cliffs, New Jersey, Prentice Hall, 1963).

⁶M. Ya. Amus'ya, N. A. Cherepkov, and L. V. Chernysheva, *Zh. Eksp. Teor. Fiz.* **60**, 160 (1971) [*Sov. Phys. JETP* **33**, 90 (1971)].

⁷A. I. Baz', Ya. B. Zel'dovich, and A. M. Perelomov, *Rasseyanie, reaktsii i res pady v nerelyativistskoĭ kvantovoi mekhanike*, Nauka, 1971 (Engl. transl. *Scattering, Reactions, and Decay in Nonrelativistic Quantum Mechanics*, Jerusalem, Israel Program for Scientific Translations, 1969).

⁸V. I. Smirnov, *Kurs vysheĭ matematiki*, Vol. 3, Nauka, 1969, Ch. 2 (Engl. transl. *A Course of Higher Mathematics*, New York, Pergamon, 1964).

⁹R. B. Barker and H. W. Berry, *Phys. Rev.* **151**, 14 (1966).

¹⁰U. Fano, *Phys. Rev.* **124**, 1866 (1961).

¹¹V. N. Ostrovskiĭ, *Zh. Eksp. Teor. Fiz.* **72**, 2079 (1977) [*Sov. Phys. JETP* **45**, 1092 (1977)].

¹²H. Bethe, *Ann. Phys. (Leipzig)* **5**, 325 (1930).

¹³R. D. Hudson and L. J. Kieffer, *Atomic Data* **2**, 205 (1971).

¹⁴M. Ya. Amusia, M. Yu. Kuchiev, S. A. Sheinerman, and S. I. Sheftel, *J. Phys. B: Atom. Molec. Phys.* **10**, L535 (1977).

¹⁵J. Fryar and J. W. McConkey, *J. Phys. B: Atom. Molec. Phys.* **9**, 619 (1976).

Translated by P. Millard

Theory of stimulated coherent emission from atoms in spatially separate optical fields

E. V. Baklanov, B. Ya. Dubetskiĭ, and V. M. Semibalamut

Institute of Heat Physics, Siberian Branch of the Academy of Sciences of the USSR, Novosibirsk
(Submitted 12 April 1978)

Zh. Eksp. Teor. Fiz. **76**, 482-504 (February 1979)

The problem of the interaction of a gas of atoms with spatially separate waves is considered. It is shown that the action of the field of two separate standing waves in a gas generates coherent radiation at distances which are multiples of the separation between the fields. The profile of the coherent emission line has a narrow resonance whose width is equal to the reciprocal of the transit times of the atoms between the field. An analysis is made of the influence of the quantization of the atomic motion (recoil effect) on the line profile. It is shown that in a wide range of the parameters the interaction of atoms with a standing wave can be regarded as a sudden perturbation. This makes it possible to solve the problem without iteration in respect of the field intensity. The coherent emission line profile is considered in the presence of high-power heterodyne laser radiation in the reception region. It is shown that it is identical with the profile of an absorption line of a weak plane probe wave localized in the region of formation of coherent radiation. The recoil effect splits the profile into a generally infinite series of components and under certain conditions the component at the line center is retained. This distinguishes fundamentally the resonance considered here from other nonlinear optical resonances. The results are given of numerical calculations of the line profile in the case when the spatially separate fields have Gaussian profiles. The optimal (in respect of the field intensity and pressure) conditions for the observation of the coherent emission effect are found. An estimate is obtained of this effect for a transition in CH_4 giving rise to emission at $\lambda = 3.39\mu$, for which the effect has been observed experimentally.

PACS numbers: 42.55.Bi, 42.50.+q, 42.55.Hq

§1. INTRODUCTION

If the lifetime of an atomic oscillator is sufficiently long, the dipole moment induced by an external field can be transported over long distances. In principle, this makes it possible to observe the emission from an atom in a region outside the range of action of the exciting field.

In the case of an ensemble of atoms with velocities exhibiting a scatter we can find the macroscopic polarization by averaging the dipole moment of an atom

over the velocities. At considerable distances from an exciting optical field the phase of the dipole moment, considered as a function of velocity, changes (in the optical frequency range) by a very large value and, consequently, the macroscopic polarization vanishes.

However, in the case of a nonlinear interaction between atoms and optical radiation the polarization may be transported in a system with spatially separate optical fields.¹ This results in generation of coherent radiation in a region where there is no exciting field.² The present paper deals with the theory of such co-